Chapter 9
Critical Issues for Circulation Modeling of Narragansett Bay and Mount Hope Bay

Changsheng Chen, Liuzhi Zhao, Geoffrey Cowles and Brian Rothschild

9.1 Introduction

Narragansett Bay is a medium-sized estuary located along the coast of the northeast United States with shoreline in both Massachusetts and Rhode Island. The bay covers 380 km^2, has an average water depth of 7.8 m, and a maximum depth of 56 m. Narragansett Bay contains three large islands—Aquidneck, Conanicut, and Prudence, all of which are oriented roughly north–south, and divide the bay into three interconnected channels—the West Passage, the East Passage, and the Sakonnet River (Fig. 9.1). The narrow linkages between these waterways control the water exchange among the various sectors of the bay. The connection to the sea is found in the southern reaches of the bay, where it opens onto the inner New England Shelf via Rhode Island Sound. In the northeast corner of the bay lies a semi-isolated shallow estuary called Mount Hope Bay. It is connected to the greater portion of Narragansett Bay through a narrow, deep channel of about 800 m in width and 25 m in depth. In view of water exchange dynamics, Narragansett Bay and Mount Hope Bay are an integrated inter-bay complex.

In recent decades, intensive short- and long-term field measurements have been made in Narragansett Bay. These observations show that regional warming has caused a dramatic increase in the stratification of the water column (Hicks, 1959; Nixon *et al*., 2004). Annual mean water temperatures in the Narragansett Bay–Mount Hope Bay system underwent an increase of 2°C from 1985 to 2001, following a decrease during 1972–1984 (Fig. 9.2a, dashed line), with a net increase of ~1.1°C overall (Fig. 9.2a, solid line). The warming trend was also observed in Woods Hole, Massachusetts (Nixon *et al.,* 2004), and in coastal waters of the northeast United States (Oviatt, 2004). The bay, which remained vertically well mixed throughout the year in 1954–1955 (Hicks, 1959), has been strongly stratified since the summer of 1990.

Changsheng Chen
The School for Marine Science and Technology, University of Massachusetts at Dartmouth, 706 South Rodney French Blvd., New Bedford, MA 02744
c1chen@umassd.edu

A. Desbonnet, B. A. Costa-Pierce (eds.), *Science for Ecosystem-based Management*.

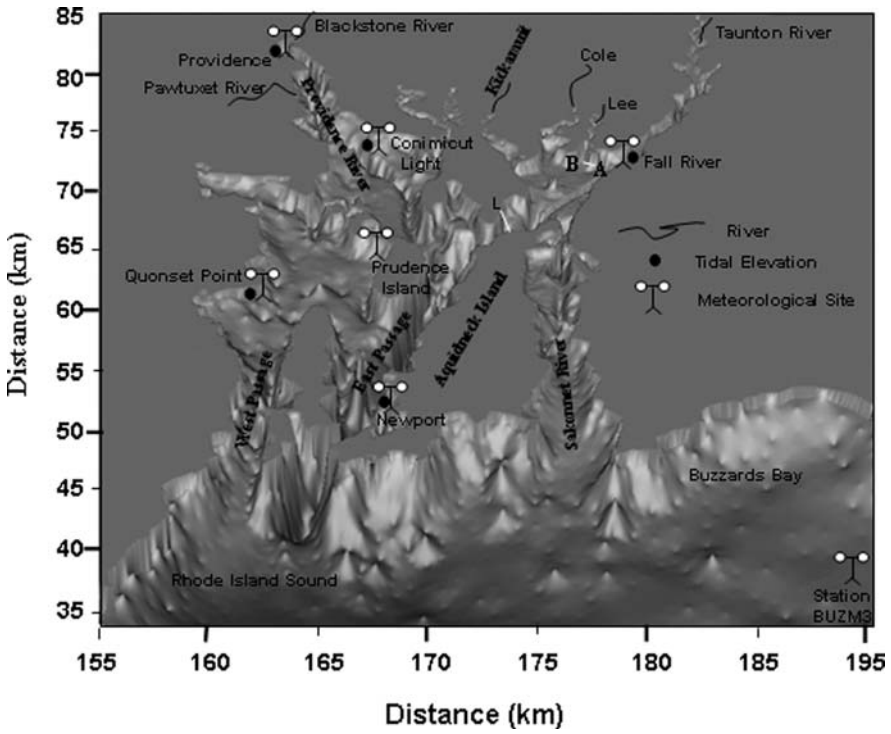

Fig. 9.1 Bathymetry of Mount Hope Bay and Narragansett Bay. L is the transect across the Narragansett Bay–Mount Hope Bay channel used to estimate water transport.

The observed increase in stratification is believed to have a negative impact on the Narragansett Bay ecosystem (Karentz and Smayda, 1998; Li and Smayda, 1998; Keller *et al.,* 1999; 2001). There is an associated reduction in vertical mixing, which leads to a reduction in oxygen exchange between the atmosphere and deeper waters of the bay. Direct observations of hypoxic (<2 mg L^{-1}) dissolved oxygen concentrations have been made in the northern bay (Bergondo *et al.,* 2005). An enlargement of the observed hypoxic area in summer from 2001 to 2002 was consistent with a significant increase in observed water stratification in the Providence River, Greenwich Bay, and the adjacent regions of Narragansett Bay (Deacutis *et al.,* 2006; Fig. 9.2c). A strong hypoxic event occurred on August 20, 2003, which caused significant mortality of menhaden, as well as many finfish, eels, crabs, soft-shell clams, and grass shrimp in Greenwich Bay, and subsequent closure of a large number of beaches in the area due to deteriorating environmental conditions (Deacutis *et al.,* 2006).

The warming tendency is also thought to advance the timing of the peak abundance of resident marine species (Sullivan *et al.,* 2001; Sullivan and Keuren, 2004), diminish eelgrass (Sullivan *et al.,* 2001), and dramatically decrease commercial fishery stocks such as winter flounder (Jeffries, 2002;

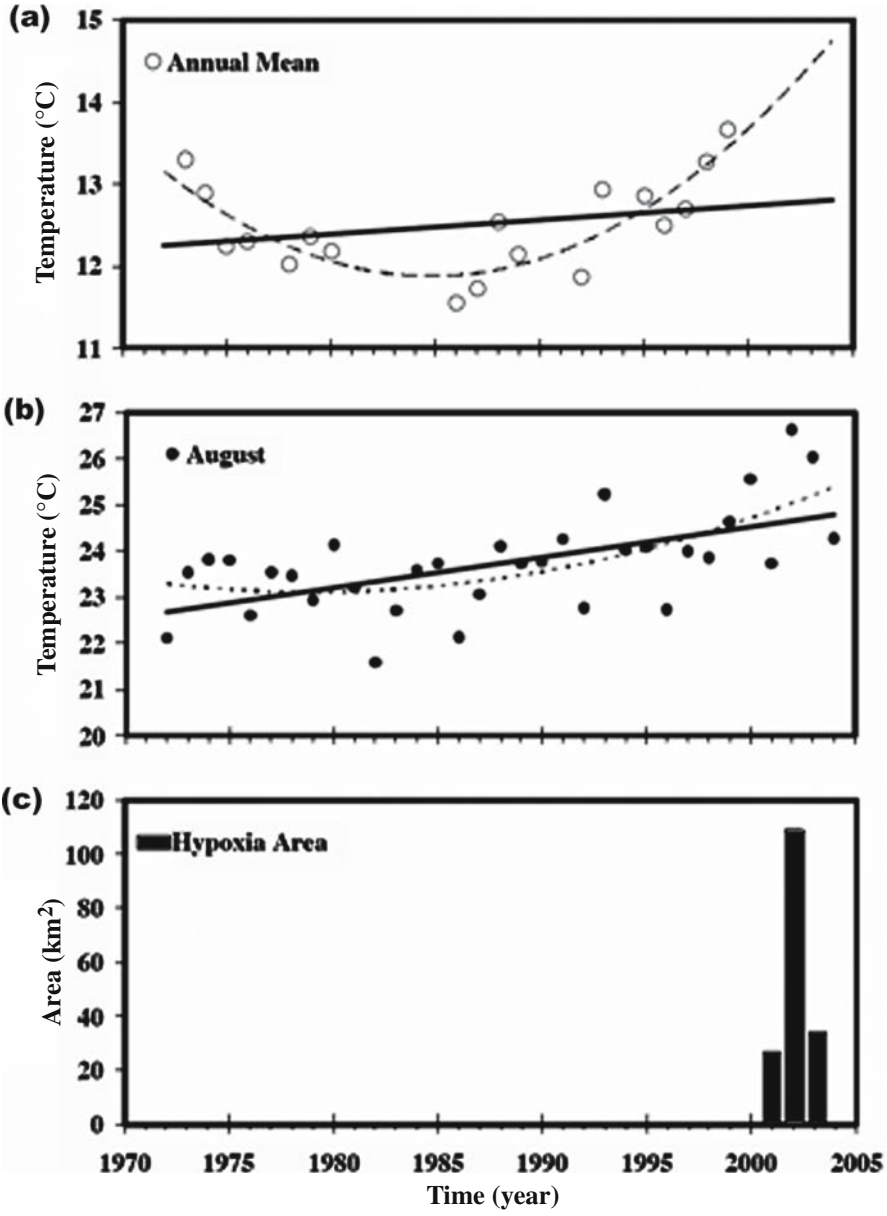

Fig. 9.2 Annual mean (upper) and August (middle) near sea surface water temperatures measured in Narragansett Bay–Mount Hope Bays from 1970–2001 and the area of hypoxia observed from 2001 to 2003. The warming trend shown in this figure is the same as that measured at Woods Hole by Nixon *et al.* (2004).

Nixon *et al.,* 2004). The winter-spring phytoplankton bloom, which normally occurs in Narragansett Bay, has not occurred in the recent warm winters (Oviatt, 2004), implying that warming in coastal waters may cause a permanent change in the phytoplankton seasonal cycle. This can, in turn, cause significant changes at higher trophic levels. These hypoxic events will lead to better evaluation of the effects of potential long-term temperature trends on the bay's ecosystem.

A direct anthropogenic warming influence on Mount Hope Bay is the Brayton Point power station, located at the northern end of the bay. Water is drawn from Mount Hope Bay, used for cooling at the facility, and discharged back into Mount Hope Bay at a higher temperature. The inflow temperature ranges from 7°C in winter to 26°C in late summer, and the discharge, about 40 $m^3 s^{-1}$, has a temperature range from 12°C in winter to 31°C in late summer.

Hypoxia has been more serious in upper Narragansett Bay and the Providence River than in Mount Hope Bay (a region with higher heating) in summer. The reason for this discrepancy lies in differences in the relative balance of physical and biological processes that lead to hypoxia in these two shallow bays. From the power station cooling system, water is discharged into Mount Hope Bay as a strong jet; it is unclear if this may lead to an increase in vertical stratification through the introduced buoyancy flux or a decrease through enhanced mixing.

In the interest of evaluating and monitoring the potential impacts of ecosystem changes in Narragansett Bay, an observational network, which includes moorings and monthly ship surveys, has been developed through a cooperative effort from the Rhode Island Department of Environmental Management, Rhode Island Division of Water Resources, The Narragansett Bay National Estuarine Research Reserve, the Narragansett Bay Commission, the University of Rhode Island, and Roger Williams University. The *in situ* water temperature, salinity, nutrients, dissolved oxygen, and chlorophyll *a* data recorded from this network help to monitor the large-scale physical and ecological conditions in the bay. While there is a clear need to focus on monitoring ecosystem change, due to the temporal and spatial sparseness of these observations, there is a limitation on the physical features that these measurements are able to resolve (Zhao *et al*., 2006). If, however, a coastal ocean model is used in conjunction with the observation network, a comprehensive analysis of the complex, temporally varying, coupled physical and biological dynamics in Narragansett Bay can be made. The underlying physical causes of ecosystem variability will be better understood, increasing the effectiveness of management and planning strategies.

This chapter focuses on the capabilities required by such a model to resolve the physical processes underlying change in the Narragansett Bay–Mount Hope Bay ecosystem. We first review the physical forcing that generates local circulation and stratification, and then present some results of modeling process studies to elucidate the numerical capabilities required to resolve detailed

circulation and water exchange, focusing on transport between Narragansett Bay and Mount Hope Bay.

9.2 Physical Forcing

Short-term circulation variability in Narragansett Bay is driven primarily by tides, local sea breezes and synoptic winds, and seasonally modified river discharge. Long-term variability in the physical environment derives from changes in freshwater runoff and wind patterns linked to decadal scale atmospheric variability, including the well-known North Atlantic Oscillation (NAO), as well as long-term trends in regional water temperature.

Tidal forcing in Narragansett Bay–Mount Hope Bay is dominated by the semidiurnal M_2 tidal constituent, which accounts for 70–80% of the total energy in bay currents, and generates most of the near-shore vertical mixing (Gordon and Spaulding, 1987; Spaulding and White, 1990; Kincaid, 2006; Zhao *et al.,* 2006). For fortnightly and monthly variations of tidal motion, N_2, S_2, K_1, and O_1 tidal constituents need to be included, although ratios of N_2 to M_2 and S_2 to M_2 are only 0.25 and 0.2, respectively, and ratios of K_1 to M_2 and O_1 to M_2 are less than 0.15 (Zhao *et al.,* 2006). Tidal waves in this region propagate into Narragansett Bay–Mount Hope Bay from the inner New England Shelf. The M_2 amplitude of the wave is about 46–48 cm at the entrance of the bay, and about 58–59 cm at the northern end (Fig. 9.3). Co-phase lines are oriented northeast–southwest, with a phase difference of about 8° between the entrance and the northern reaches. Due to Coriolis effects, tidal elevation is slightly higher on the right side coast (east) than on the left side coast (west). Tidal variation in Mount Hope Bay is mainly controlled by wave propagation through the narrow Narragansett Bay–Mount Hope Bay channel. For a given latitude, the tidal phase in Mount Hope Bay lags that of upper northwest Narragansett Bay by only 1–2°.

The amplitude of the tidal currents in Narragansett Bay–Mount Hope Bay varies significantly with location due to variable bathymetry and local acceleration driven by narrow passages between the islands in the bay. Tidal ellipses are generally oriented parallel to local isobaths (Fig. 9.4). Eddies are generated by the separation of tidal currents in diverging channels and around islands and coastal headlands. In deep channels and passages, the maximum speed of currents may exceed 100 cm s^{-1} (Zhao *et al.,* 2006).

Freshwater discharge into the bay ecosystem derives primarily from three major rivers: the Taunton River at the northeastern head of Mount Hope Bay, and the Blackstone and Pawtuxet Rivers at the northwestern head of Narragansett Bay. These rivers drain approximately 4,500 km^2 of adjacent watershed in Massachusetts and Rhode Island (Pilson, 1985). The annual average discharge rate (based on outflow data from 1929–2003) is about 14 m^3 s^{-1} for the Taunton River, 22 m^3 s^{-1} for the Blackstone River, and 10 m^3 s^{-1} for the

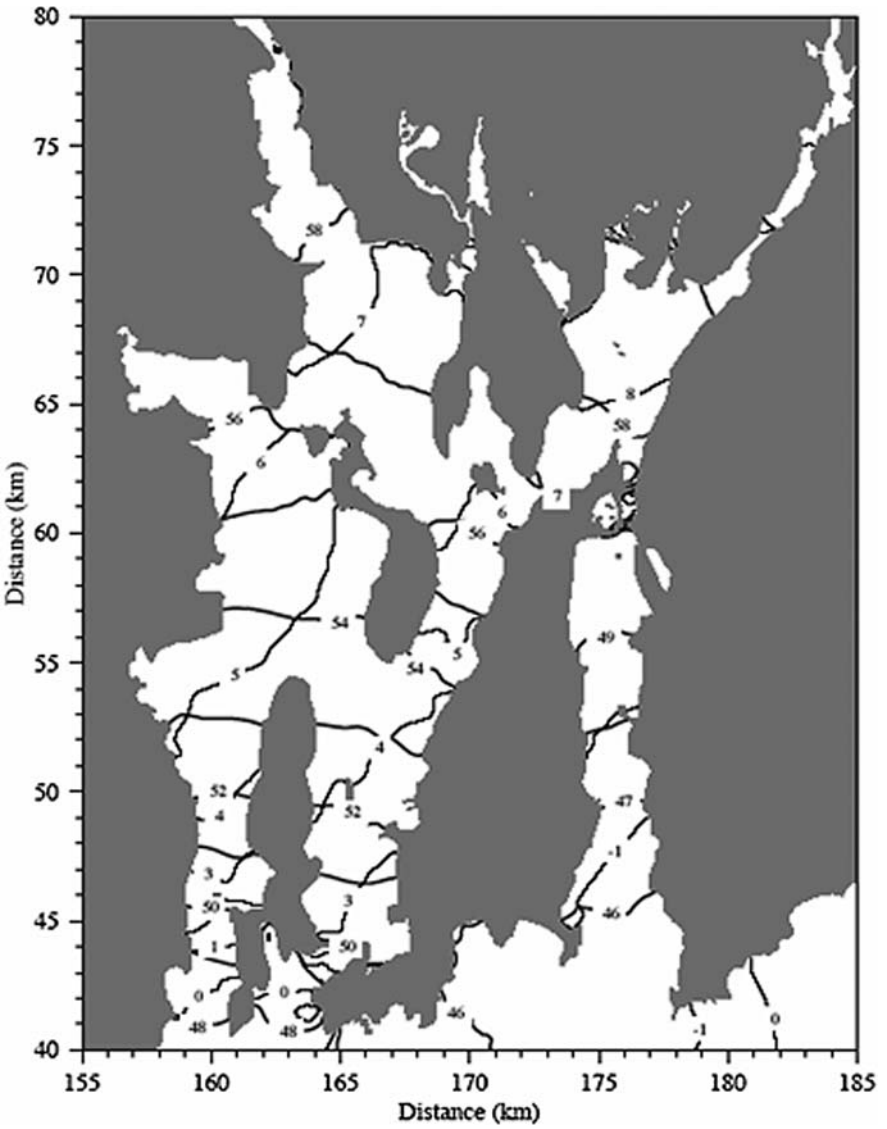

Fig. 9.3 Co-tidal chart of the model-predicted M_2 tidal elevation. Heavy solid line: Co-amplitude (cm) and thin solid line: co-phase (°G). This figure is adopted directly from Zhao *et al*. (2006).

Pawtuxet River (Fig. 9.5). Peaks in river discharge are generally found in December and March, with a monthly-averaged volume flux of approximately 40 $m^3 s^{-1}$. There is significant inter-annual variability in the timing and magnitude of the peak discharge rate. In 1972, for example, the maximum discharge rate in the Blackstone exceeded 60 $m^3 s^{-1}$ in December and 80 $m^3 s^{-1}$ in March.

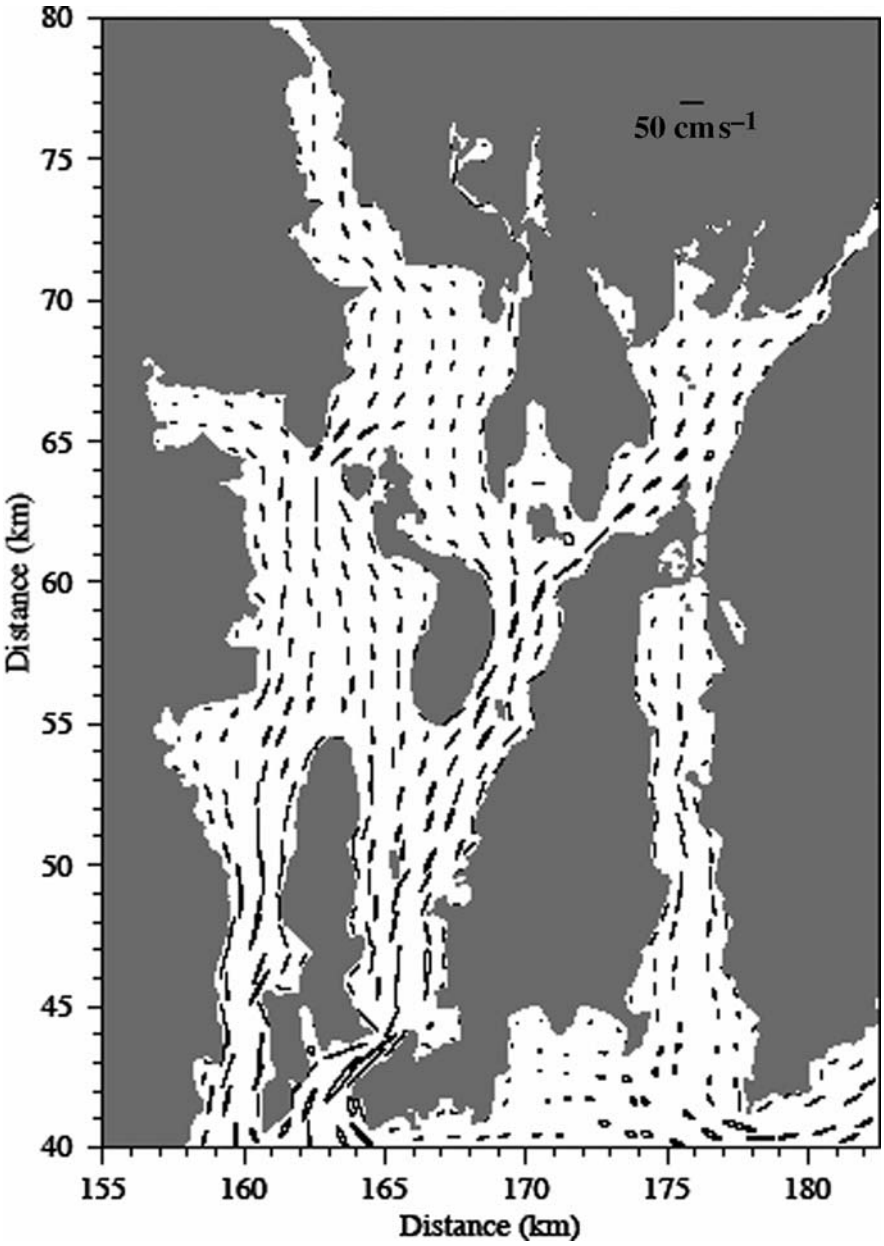

Fig. 9.4 The M_2 tidal current ellipse chart for selected sites from the model results. This figure is adopted directly from Zhao *et al*. (2006).

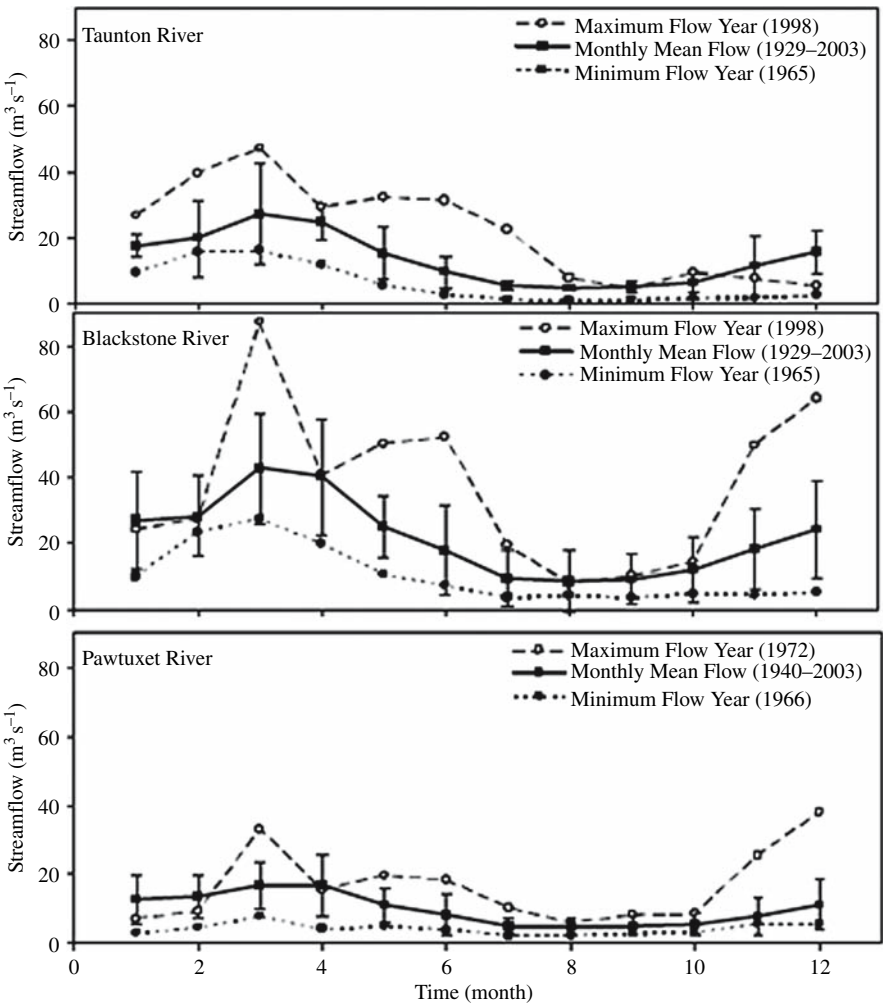

Fig. 9.5 Monthly freshwater discharges for the Taunton, Blackstone, and Pawtuxet Rivers. The data used for this analysis were downloaded from the USGS website.

That year also featured an additional late spring peak in June exceeding 40 $m^3\ s^{-1}$. In 1965, a year of anomalously low discharge, the maximum discharge rate in the Blackstone was only about 20 $m^3\ s^{-1}$.

River discharge has a direct impact on the seasonal variation of near-surface stratification and nutrient loading into the bay (Weisberg, 1976; Weisberg and Sturges, 1976; Kremer and Nixon, 1978). Buoyancy-induced flow in Narragansett Bay–Mount Hope Bay is driven mainly by freshwater discharge from rivers.

Wind forcing in Narragansett Bay–Mount Hope Bay is highly variable, both temporally and spatially. While synoptic-scale (2–5 days) fluctuations are

Table 9.1 Correlation coefficients of the wind velocity at six meteorological measurement stations in the Narragansett Bay–Mount Hope Bay system.

u v	Providence	Conimicut Light	Potter Cove	Quonset Point	Newport	Buzzards Bay
Providence	1	0.64	0.63	0.57	0.49	0.56
Conimicut Light	0.88	1	0.73	0.47	0.40	0.66
Potter Cove	0.85	0.86	1	0.68	0.65	0.73
Quonset Point	0.89	0.94	0.91	1	0.73	0.64
Newport	0.81	0.85	0.89	0.90	1	0.63
Buzzards Bay	0.75	0.82	0.83	0.83	0.90	1

u = the cross-shelf component; v = the along-shelf component.

driven by large-scale weather patterns, sea breezes dominate the daily variation. A correlation analysis of wind direction from measurement sites in Newport, Fall River, Conimicut Point, Providence, and Quonset Point found that wind is highly correlated ($r = 0.75$–0.94) along the coastal direction, but has reduced correlation in the cross-coastal direction (Table 9.1). These findings are consistent with the notion that local sea breeze, generally from the southwest, is a significant component of wind variability over Narragansett Bay. This supports the result from correlation analysis that wind variability in Narragansett Bay–Mount Hope Bay is controlled by short-term fluctuations induced by local sea breeze as well as the episodic passage of atmospheric fronts.

9.3 An Unstructured Grid Narragansett Bay–Mount Hope Bay Model

In the last decade, the basic circulation in Narragansett Bay–Mount Hope Bay has been examined using various oceanographic models (Gordon and Spaulding, 1987; Swanson and Jayko, 1987; Spaulding *et al.,* 1999), all of which were discretized using structured grids. Gordon and Spaulding (1987) applied a traditional finite-difference model to simulate the tidal motion in Narragansett Bay. Forced by the M_2 and M_4 tidal constituents at open boundaries, their model successfully reproduced the M_2- and M_4-induced tidal amplitude and phase in good agreement with tidal gauge observations. A similar effort was made by Spaulding *et al.* (1999), who included 37 tidal constituents for the purpose of improving the accuracy of tidal simulation. Scientists at Applied Science Associates, Inc. (ASA) applied a curvilinear structured grid coastal ocean model to evaluate the impact of warm water discharge on stratification and circulation in Mount Hope Bay (Swanson and Jayko, 1987). While

the curvilinear coordinate model provided improved resolution of the coastline relative to previous studies using Cartesian coordinate models, limitations in their model resolution led to the diffusion of modeled plume. Spaulding and Swanson provide a greater account on the above in Chapter 8.

Most coastal ocean models are based on the same governing equations—the hydrostatic primitive equations (HPE). Driven by the same external forcing, these models should converge toward the same solution as the grid resolution is increased. Ultimately, however, the efficiency by which the models can resolve relevant processes depends on the spatial order of accuracy and the mesh type used for discretization (Chen *et al.,* 2007). The regions at Narragansett Bay–Mount Hope Bay are separated by narrow openings that control the exchange of water among them. The inability to resolve transport through these links will degrade the overall simulation of bay circulation.

A model for resolving the fundamental processes that control circulation in Narragansett Bay–Mount Hope Bay requires: (1) grid flexibility to resolve complex coastline and bathymetry; (2) mass conservation to accurately simulate water, heat, salt, and nutrient transports; (3) proper parameterization of vertical mixing to simulate tidal and wind mixing; and (4) the capability to assimilate observed quantities as real-time atmospheric and coastal ocean measurements become more easily available.

Funded by the Brayton Point Power Plant, the Marine Ecosystem Dynamics Laboratory at the University of Massachusetts-Dartmouth has developed an integrated model for the Narragansett Bay–Mount Hope Bay region. The major components of this system include: (1) a meso-scale atmospheric model (MM5) (Chen *et al.,* 2005), (2) the unstructured-grid Finite-Volume Coastal Ocean circulation Model (FVCOM), and (3) a lower trophic-level food web model. FVCOM is the key component of this integrated system; it solves the hydrostatic primitive equations on unstructured triangular meshes using finite-volume discretization of spatial derivatives (Chen *et al.,* 2003; Chen *et al.,* 2006a,b). Furthermore, it is fully parallelized for efficient multiprocessor execution (Cowles, 2007). Like other coastal models, FVCOM uses the modified Mellor and Yamada level 2.5 (MY-2.5) and Smagorinsky turbulent closure schemes for vertical and horizontal mixing, respectively (Smagorinsky, 1963; Mellor and Yamada, 1982; Galperin *et al.,* 1988), and a sigma coordinate to follow bottom topography. The General Ocean Turbulence Model (GOTM) (Burchard *et al.,* 1999; Burchard, 2002) has been added to FVCOM to provide additional vertical closure schemes. The wet/dry point-treatment method may be incorporated to simulate the flooding/drying process on inter-tidal wetlands. Unlike the existing coastal finite-difference and finite-element models, FVCOM can be solved numerically by calculating fluxes resulting from discretization of the integral form of governing equations on an unstructured triangular grid. This approach combines the best features of finite-element methods (grid flexibility) and finite-difference methods (numerical efficiency and code simplicity), and provides a good numerical representation of momentum, mass, salt, heat, and tracer conservation. An advantage of an unstructured grid model is that grid

density can vary spatially, and thus the mesh can be tailored locally to resolve critical processes as well as the complex coastline. This new model is extremely well suited to regions with complex coastlines and bathymetry, meets the requirements described above, and has been successfully applied to simulate circulation in Narragansett Bay–Mount Hope Bay for the last two years (Zhao *et al.,* 2006).

For circulation modeling in Narragansett Bay, a mesh covering the entire Narragansett Bay–Mount Hope Bay region is used (Fig. 9.6). The open boundary of the computational domain forms an arc that runs from Rhode Island Sound to Buzzards Bay. The mesh used here has a variable horizontal grid scale, which ranges from a minimum of 10 m in the northern reaches of Narragansett Bay and Mount Hope Bay to a maximum of 5 km near the open boundary. The vertical coordinate is discretized using 30 equally-spaced layers.

FVCOM has been successfully used to simulate the tidal, river-discharge, and wind-driven currents and the thermal plume in Narragansett Bay–Mount Hope Bay. The model results were validated with direct comparisons to relevant field measurement data. A summary of the model results can be found in Zhao *et al.* (2006).

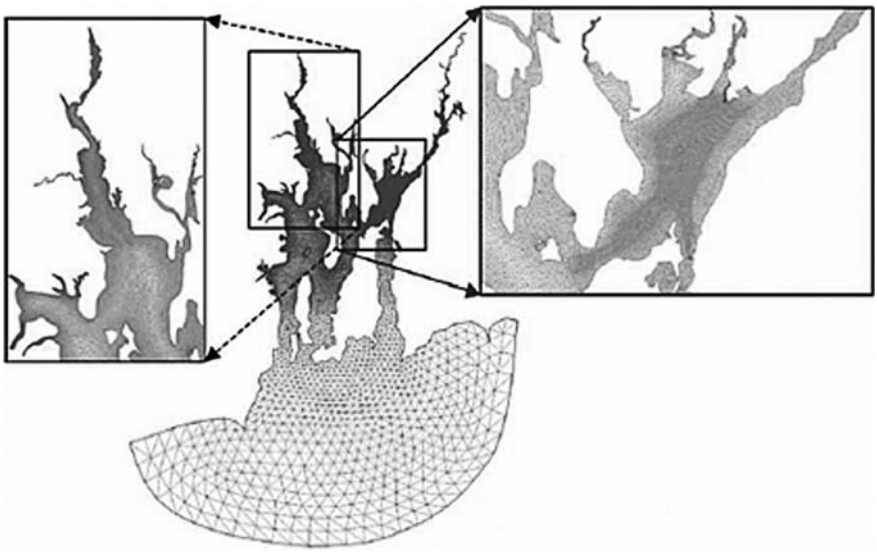

Fig. 9.6 Unstructured grid of the Narragansett Bay–Mount Hope Bay finite-volume coastal ocean model (FVCOM). The horizontal resolution ranges from 10–50 m in upper Narragansett Bay to 100 m over the shelf. This is the new configuration modified from our existing FVCOM to match the dynamic requirements to correctly resolve the tidal flushing and current separation as well as the river plume. 31-sigma levels are used in the vertical.

9.4 Numerical Process Studies in Narragansett Bay–Mount Hope Bay

Process studies were carried out using the FVCOM model to determine the numerical parameters required for resolving principle circulation in Mount Hope Bay, and the extent of the thermal plume generated by the cooling water discharge. These studies included investigations of initial conditions, horizontal and vertical grid resolution, and model time step. Although often disregarded, grid resolution studies are an important component of any model validation effort. The expected resolution is problem dependent, and a careful grid convergence study is necessary to determine proper grid scales.

9.4.1 Case 1: Tidal Flushing in the Narragansett Bay–Mount Hope Bay Channel

Narragansett Bay, Mount Hope Bay, and the Sakonnet River Narrows form an integrated dynamic system. Water exchange between greater Narragansett Bay and Mount Hope Bay occurs principally through the narrow neck separating the two waterbodies. The maximum tidal current through this opening can exceed 100 cm s^{-1}, and current separation on the diverging (downstream) side of the opening generates flow reversal, forming eddies on each side of the current jet around the time of maximum flood (Zhao *et al.,* 2006). These eddies were evident in the measurements made by Kincaid (in press) in the Narragansett Bay–Mount Hope Bay channel. Due to interactions between Narragansett Bay–Mount Hope Bay and Mount Hope Bay–Sakonnet River Narrows water exchanges, water transport in Mount Hope Bay–Sakonnet River Narrows leads the Narragansett Bay–Mount Hope Bay channel by $\sim 90^{\circ}$, even though the transport volume is smaller by a factor of five (Zhao *et al.,* 2006). This phase lead was also observed by Kincaid (2006).

To resolve circulation through these narrow openings, including the development and dissolution of time-dependent lee side eddies, a model must have adequate mesh spacing to resolve the detailed geometries of these narrow necks. The Sakonnet River Narrows are 1,500 m in length and 7 m in mean water depth, and are characterized by two necks with a width of about 70 m at Sakonnet River Bridge and 120 m at Stone Bridge, respectively (Fig. 9.1). The previous models used in this region were discretized using a curvilinear coordinate system (Gordon and Spaulding, 1987; Swanson and Jayko, 1987; Spaulding *et al.,* 1999; Sullivan and Kincaid, 2001). With a horizontal resolution of $\sim$200 m, these models were not able to resolve the geometry of the two narrow necks in the Sakonnet River Narrows, and thus we do not expect that they could simulate a realistic water exchange process between Narragansett Bay and Mount Hope Bay. By using flexible unstructured grids, FVCOM is able to

adapt to local scales using variable grid resolution, resulting in a more efficient use of grid cells and enabling the model to resolve tidal-driven water transport processes between Narragansett Bay and Mount Hope Bay.

The current separation observed in our process studies was not reported in previous modeling work. This is likely because the 200-m grid scale used in the previous work was not sufficient to resolve the lateral shear of current jet in the narrow (800 m) Narragansett Bay–Mount Hope Bay channel. After observing the implications of resolution on the computed water exchange, we sought to determine the necessary grid scale for the Narragansett Bay–Mount Hope Bay channel.

Using nominal mesh spacing of 50 and 200 m in the Narragansett Bay–Mount Hope Bay channel, we examined the temporal response of circulation in the channel generated by tidal forcing at the open boundary. In a higher resolution (50 m), the model is able to predict current separation and subsequent eddy shedding. During flood, water that originates from the East Passage flows around Hog Island, merges on the eastern side of the island, and then flushes into Mount Hope Bay through the deep channel (Fig. 9.7a). Current separation on the lee side of the channel generates eddies on each side of the current jet around the time of maximum flood. The eddy on the eastern side enlarges, and its center migrates northeastward after the time of maximum flood, while the eddy on the western side intensifies as a result of an increase of the southward along-coastal tidal flow during the late flood phase. During the ebb period, when tidal currents are reversed, current separation occurs on the Narragansett Bay side of the Narragansett Bay–Mount Hope Bay channel. In this case, the eddy on the northern coast forms around the time of maximum ebb, while the eddy on the southern coast forms several hours after the maximum ebb (Fig. 9.7b).

With a low-resolution (200 m) grid, the model predicts strong tidal currents during the flood and ebb period through the Narragansett Bay–Mount Hope Bay channel. During flood, an eddy clearly forms on the eastern side of the current jet, but there is no clear evidence of flow reversal on the western side (Fig. 9.8a). During the ebb period, no significant eddy shedding was resolved on the lee side of tidal flushing in Narragansett Bay (Fig. 9.8b). The lateral shear of tidal current was much larger in high resolution than in low resolution (Fig. 9.9). Resolving the lateral shear of tidal current jet is critical for the prediction of timing and strength of current separation in a diverging channel (Stommel and Farmer, 1952; Wells and Heijst, 2003).

9.4.2 Case 2: Thermal Plume

One of main features driving the circulation and hydrography in Mount Hope Bay is the thermal plume resulting from cooling water discharge from the Brayton Point Power Plant. The temporal and spatial structure of this plume

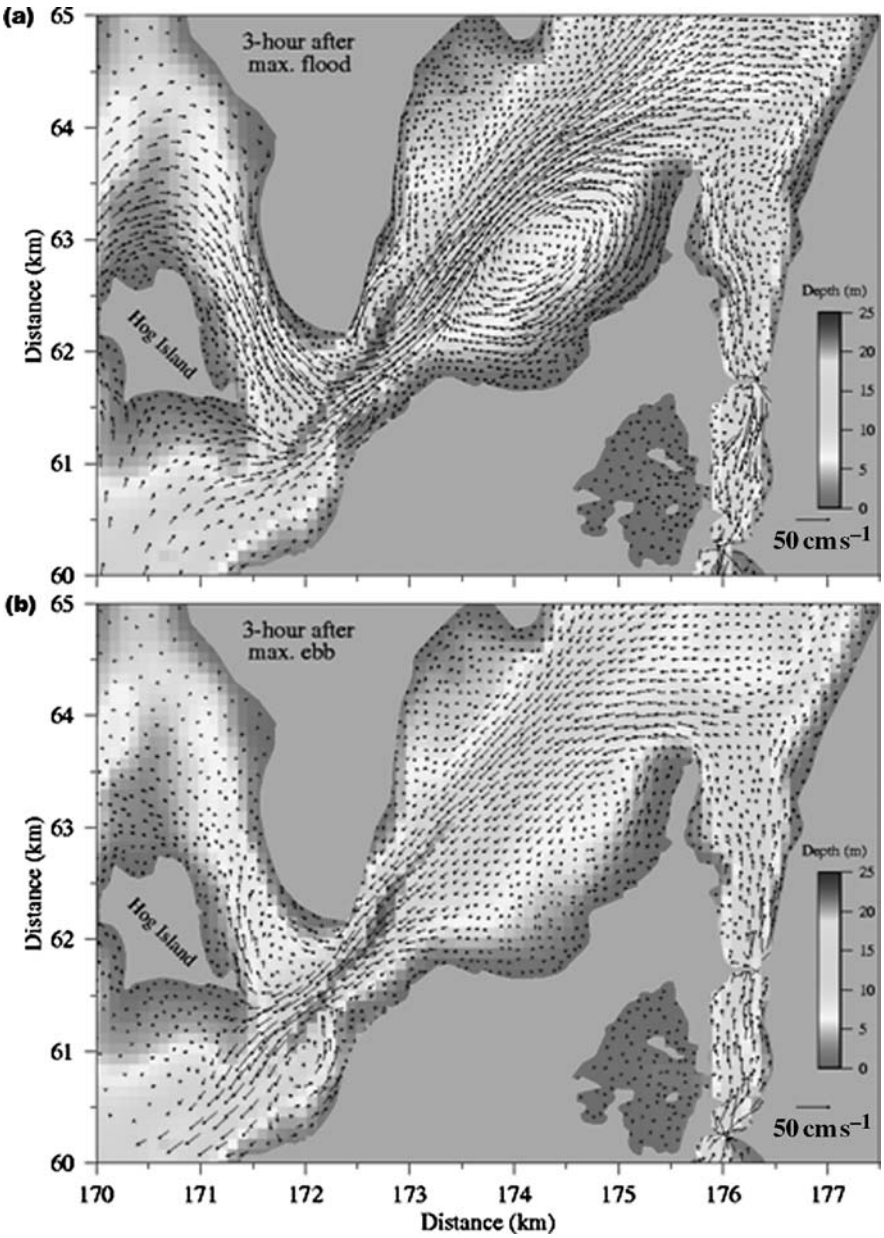

Fig. 9.7 The distributions of the near-surface tidal current 3 h after the maximum flood (a) and 3 h after the maximum ebb (b) in the southern part of the Mount Hope Bay–Narragansett Bay–Sakonnet River regions for the model run with a horizontal resolution of 50 m in the Narragansett Bay–Mount Hope Bay channel. The image shows the bathymetry with depth scales from 0 to 25 m. The number of current points is reduced in the high-resolution region to improve figure clarity.

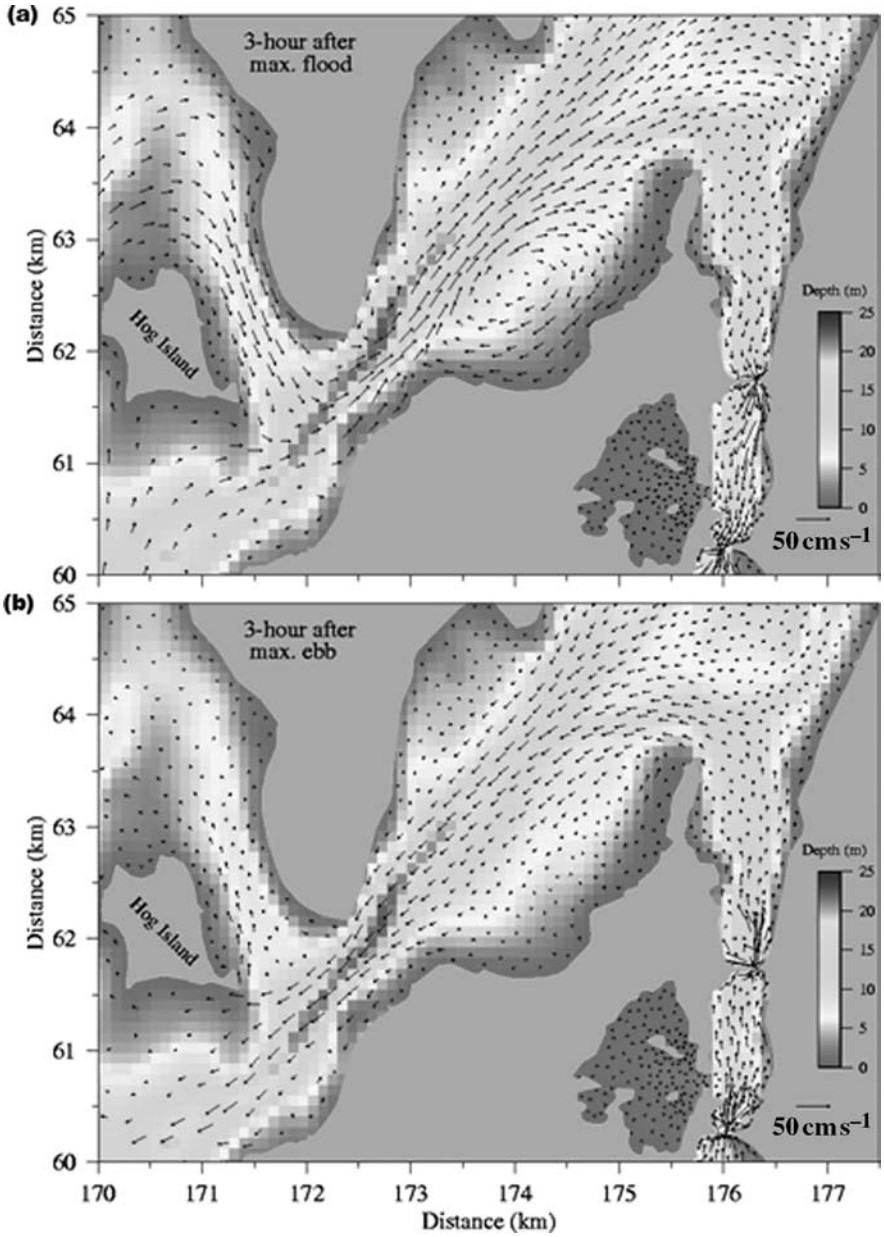

Fig. 9.8 The distributions of the near-surface tidal current 3 h after the maximum flood (a) and 3 h after the maximum ebb (b) in the southern part of the Mount Hope Bay–Narragansett Bay–Sakonnet River regions for the model run with a horizontal resolution of 200 m in the Narragansett Bay–Mount Hope Bay channel. The image shows the bathymetry with depth scales from 0 to 25 m. The number of current points is reduced in the high-resolution region to improve figure clarity.

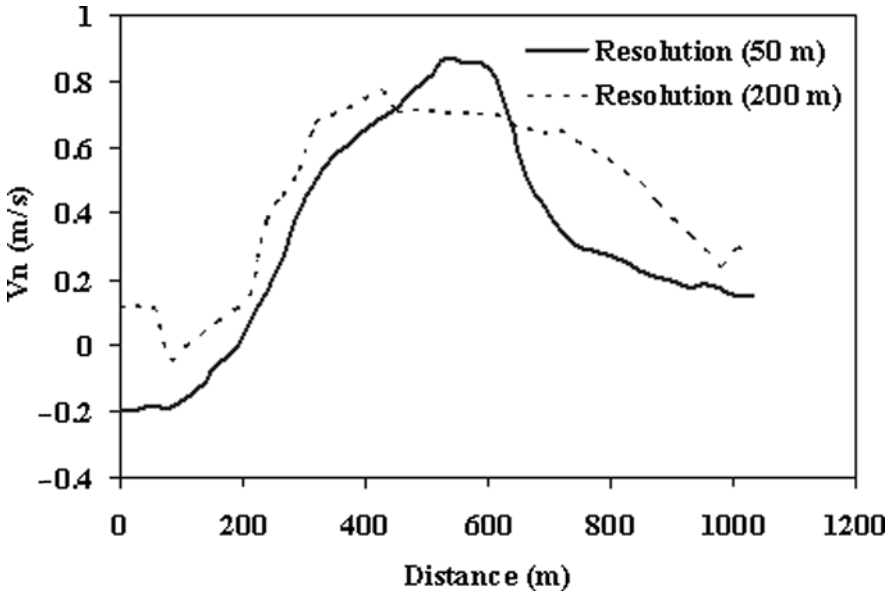

Fig. 9.9 The distribution of the along-isobaths tidal current on the transect L (shown in Fig. 9.1) for the model runs with horizontal resolution of 50 and 200 m in the channel, respectively.

was observed using thermal imaging from an aircraft in September 1998 by scientists at Brown University. The images were taken through the course of one tidal cycle; they clearly show that the basic plume structure is a narrow jet that meanders widely through tidal motion. To map the vertical and lateral structure of the thermal plume, a team of scientists from the University of Massachusetts-Dartmouth (UMASSD) and Woods Hole Oceanographic Institution (WHOI) conducted a high-resolution tow-yo CTD/ADCP survey with repeated tracks across the thermal plume on August 19, 2005, a time of perigee spring tides. Two drifters with portable global positioning system recorders were released at the time of maximum ebb tidal current at the center of the thermal plume to track the trajectory of discharge water. The CTD/ADCP data showed that the plume was a narrow current jet with a width of ~30–40 m, a vertical scale of ~2 m and a maximum velocity exceeding 60 cm s^{-1} during the ebb. A weak return flow was detected on the western side of the plume jet. This evidence was supported by the trajectories of two drifters, which turned clockwise and moved toward the western coast of Mount Hope Bay.

The thermal plume influences the circulation in Mount Hope Bay through a contribution of kinetic energy and buoyancy. Failure to resolve the plume and associated density gradients can lead to unrealistic modeling of buoyancy-driven circulation and stratification. In the previous efforts to study the plume using a curvilinear mesh with inadequate resolution, the plume size

was over-predicted, and consequently an exaggeration of the area of influence of warm water (Swanson and Jayko, 1987).

To examine the sensitivity of model-simulated thermal plume to grid spacing, the FVCOM Narragansett Bay–Mount Hope Bay model was executed using horizontal resolutions of 50, 25, 10 and 5 m in northern Mount Hope Bay. The associated impact on water exchange between Mount Hope Bay and Narragansett Bay was also evaluated. For these experiments, the initial conditions of water temperature and salinity were specified using an August climatologic field constructed from historical databases spanning the period 1959–2005. For the same initial conditions (temperature and salinity) and forcing (thermal flux from the power plant and tides), the width of the thermal plume becomes smaller as horizontal resolution increases. Grid convergence is reached when the horizontal resolution is reduced to 10 m. The model comparison results clearly show that insufficiency in horizontal resolution can lead to an over-estimation of lateral diffusion, thus exaggerating the region of influence of heat flux from the power station.

An accurate determination of the contribution of plume heat to the overall temperature in Mount Hope Bay requires an accurate prediction of water exchange between Mount Hope Bay and the adjacent regions. Kincaid (in press) used repeated ADCP transects across the Narragansett Bay–Mount Hope Bay channel to estimate volume transport. He measured the water transport to be $7.5 \times 10^3\,m^3\ s^{-1}$ at the current peak of spring tide. The FVCOM-modeled volume transport for the same phase in spring tide was $5.2 \times 10^3\ m^3\ s^{-1}$, $6.2 \times 10^3\ m^3\ s^{-1}$, and $6.7 \times 10^3\ m^3\ s^{-1}$ for the cases with horizontal resolutions of 50, 10, and 5 m in the thermal plume area, respectively. Inadequate resolution reduces the exchange of heat between Mount Hope Bay and Narragansett Bay, and can lead to incorrect conclusions on the impact of the thermal plume on Mount Hope Bay.

9.5 Summary

A recent increase in the frequency of hypoxic events in Narragansett Bay reinforces the need to understand the causes of these harmful ecological conditions, as well as the reasons for their observed spatial variability. A well-calibrated model used in concert with an appropriate observation network can elucidate some of the underlying physical mechanisms of ecosystem change in the Narragansett Bay–Mount Hope Bay ecosystem. The bay is divided naturally into subregions separated by narrow channels, and modeling the general circulation of the bay requires resolving the interchange through these narrow channels.

Process-oriented modeling experiments were used to examine the grid resolution required for resolving the exchange of water between Narragansett Bay and Mount Hope Bay, as well as the thermal plume generated by the cooling

water discharge of the Brayton Point power station. Results of these experiments indicate that, due to insufficient computing, past modeling efforts lacked the necessary mesh resolution to capture complex circulation generated by tidal forcing through the Narragansett Bay–Mount Hope Bay channel, or the extent of the thermal plume. With an unstructured grid approach, the flexibility in grid resolution allows efficient placement of mesh cells as well as accurate rendering of the detailed coastline. In combination with recent advances in computing, the unstructured grid method offers the potential for grid-converged solutions of the processes controlling circulation in the ecosystem.

It should be pointed out here that the model results for tidal flushing presented in this chapter were based on numerical experiments conducted without river discharge or surface forcing being considered. Because eddies generated by tidal flushing through the Narragansett Bay–Mount Hope Bay channel occur in the shallower area (where water depth is <4 m), they may not be observed when wind is present. The wind in Narragansett Bay and Mount Hope Bay can vary significantly during the day due to local sea breeze. In such shallow areas, wind-driven current is usually in the same direction of surface wind stress (Chen, 2000). Eddies can disappear when the wind-induced current is larger than the tidal-induced eddy current.

Acknowledgment This research is supported by a private research fund awarded by the Fall River Mount Hope Bay Power Plant and Rhode Island Sea Grant under contract number NA040AR4170062. We would like to thank Dr Robert Beardsley at Woods Hole Oceanographic Institution (WHOI) for his encouragement as well as his collaboration in the development of FVCOM, and Jim Churchill (WHOI) for conducting the drifter experiments in the August 2005 Mount Hope Bay survey. We would also like to thank the members of the Marine Ecosystem Dynamics Modeling (MEDM) Laboratory at the School for Marine Science and Technology, University of Massachusetts-Dartmouth for their support in FVCOM development. This paper is #06-1102 in the SMAST Contribution Series, School for Marine Science and Technology, University of Massachusetts-Dartmouth.

References

Bergondo, D.L., Kester, D.R., Stoffel, H.E., and Woods, W. 2005. Time-series observations during the low sub-surface oxygen events in Narragansett Bay during summer 2001. *Marine Chemistry* 97:90–103.

Burchard, H. 2002. Applied Turbulence Modeling in Marine Waters. New York: Springer. 215 pp.

Burchard, H., Bolding, K., and Villarreal, M.R. 1999. GOTM–A general ocean turbulence model. Theory, applications and test cases. Technical Report, EUR 18745 EN, European Commission.

Chen, C. 2000. A modeling study of episodic cross-frontal water transports over the inner shelf of the South Atlantic Bight. *Journal of Physical Oceanography* 30:1722–1742.

Chen, C., Liu, H., and Beardsley, R. 2003. An unstructured grid, finite-volume, three-dimensional, primitive equations ocean model: application to coastal ocean and estuaries. *Journal of Atmospheric and Oceanic Technology* 20(1):159–186.

Chen, C., Beardsley, R.C., Hu, S., Xu, C., and Lin, H. 2005. Using MM5 to hindcast the ocean surface forcing fields over the Gulf of Maine and Georges Bank region. *Journal of Atmospheric and Oceanic Technology* 22(2):131–145.

Chen, C., Beardsley, R.C., and Cowles, G. 2006a. An unstructured grid, finite-volume coastal ocean model (FVCOM) system. Special Issue "Advances in Computational Oceanography", *Oceanography* 19(1):78–89.

Chen, C., Cowles, G., and Beardsley, R.C. 2006b. An unstructured grid, finite-volume coastal ocean model: FVCOM User Manual. Second Edition. SMAST/UMASSD Technical Report-06-0602, pp. 315.

Chen, C., Huang, H., Beardsley, R.C., Liu, H., Xu, Q., and Cowles, G. 2007. A finite-volume numerical approach for coastal ocean circulation studies: comparisons with finite-difference models. *Journal of Geophysical Research* 112.

Cowles, G.W. 2007. Parallelization of the FVCOM Coastal Ocean Model. International Journal of High Performance Computing Applications, in press.

Deacutis, C.F., Murray, D.W., Prell, W.L., Saarman, E., and Korhun, L. 2006. Hypoxia in the Upper Half of Narragansett Bay, RI during August 2001 and 2002, *Northeast Naturalist* 13(Special Issue 4):173–198.

Galperin, B., Kantha, L.H., Hassid, S., and Rosati, A. 1988. A quasi-equilibrium turbulent energy model for geophysical flows. *Journal of Atmospheric Sciences* 45:55–62.

Gordon, R., and Spaulding, M.L. 1987. Numerical simulation of the tidal and wind driven circulation in Narragansett Bay. *Estuarine, Coastal, and Shelf Science* 24:611–636.

Hicks, S.D. 1959. The physical oceanography of Narragansett Bay. *Limnology and Oceanography* 4:316–327.

Jeffries, P. 2002. Rhode Island's ever-change Narragansett Bay. *Maritimes* 41:1–5.

Karentz, D., and Smayda, T.J. 1998. Temporal patterns and variations in phytoplankton community organization and abundance in Narragansett Bay during 1959–1980. *Journal of Plankton Research* 20:145–168.

Keller, A.A., Oviatt, C.A., Walker, H.A., and Hawk, J.D. 1999. Predicted impacts of elevated temperature on the magnitude of the winter-spring phytoplankton bloom in temperate coastal waters: a mesocosm study. *Limnology and Oceanography* 44:344–356.

Keller, A.A., Taylor, C., Oviatt, C., Dorrington, T., Holcombe, G., and Reed, L. 2001. Phytoplankton production patterns in Massachusetts Bay and the absence of the 1998 winter-spring bloom. *Marine Biology* 138:1051–1062.

Kincaid, C. 2006. The exchange of water through multiple entrances to the Mt. Hope Bay estuary. *Northeast Naturalist* 13(Special Issue 4):117–144.

Kremer, J.N., and Nixon, S.W. 1978. A coastal marine ecosystem: Simulation and analysis. New York: Springer Verlag.

Li, Y., and Smayda, T.J. 1998. Temporal variability of chlorophyll in Narragansett Bay, 1973–1990. *ICES Journal of Marine Science* 55:661–667.

Mellor, G.L., and Yamada, T. 1982. Development of a turbulence closure model for geophysical fluid problem. *Reviews of Geophysics and Space Physics* 20:851–875.

Nixon, S.W., Granger, S., Buckley, B.A., Lamont, M., and Rowell, B. 2004. A one hundred and seventeen year coastal water temperature record from Woods Hole, Massachusetts. *Estuaries* 27:397–404.

Oviatt, C.A. 2004. The changing ecology of temperate coastal waters during a warming trend. *Estuaries* 27:895–904.

Pilson, M.E.Q. 1985. On the residence time of water in Narragansett Bay. *Estuaries* 8:2–14.

Smagorinsky, J. 1963. General circulation experiments with the primitive equations, I. The basic experiment. *Monthly Weather Review* 91:99–164.

Spaulding, M.L., and White, F.M. 1990. Circulation dynamics in Mt. Hope Bay and the lower Taunton River, Narragansett Bay. *In* Coastal and Estuarine Studies, Vol. 38. Cheng, R.T. (ed.) New York: Springer-Verlag.

Spaulding, M.L., Mendelsohn, D., and Swanson, J.C. 1999. WQMAP: an integrated three-dimensional hydrodynamic and water quality model system for estuarine and coastal applications. *Marine Technology Society Journal Special issue on State of the Art in Ocean and Coastal Modeling* 33(3):38–54.

Stommel, H., and Farmer, H.G. 1952. On the nature of estuarine circulation. WHOI Technical Report 52–88, 131 pp.

Sullivan, B.K., and Kincaid, C. 2001. Modeling circulation and transport in Narragansett Bay. AGU Spring Meeting Abstract, 21, OS21A05S.

Sullivan, B.K. and D.V. Keuren, 2004. Climate change and zooplankton predator-prey dynamics. Presentation at Science Symposium 2004 "State of Science Knowledge on Nutrients in Narragansett Bay". 17–18 November, Block Island, RI.

Sullivan, B.K., Van Keuren, D., and Clancy, M. 2001. Timing and size of blooms of the ctenophore *Mnemiopsis leidyi* in relation to temperature in Narragansett Bay, RI. *Hydrobiologia* 451:113–120.

Swanson, J.C. and K. Jayko. 1988. A simplified estuarine box model of Narragansett Bay. Final report prepared for the Narrangansett Bay Project and the Environmental Protection Agency, Region I. Applied Science Associates, Inc. No. 85–11. 90 pp.

US Geological Survey (USGS) 2007. *http://ma.water.usgs.gov/basins*.

Weisberg, R.H. 1976. The non-tidal flow in the Providence River of Narragansett Bay: a stochastic approach to estuarine circulation. *Journal of Physical Oceanography* 6:721–734.

Weisberg, R.H., and Sturges, W. 1976. Velocity observations in the west passage of Narragansett Bay: a partially mixed estuary. *Journal of Physical Oceanography* 6:345–354.

Wells, M.G., and Heijst, G. 2003. A model of tidal flushing of an estuary by dipole formation, *Dynamics of Atmosphere and Oceans* 37:223–244.

Zhao, L., Chen, C., and Cowles, G. 2006. Tidal flushing and eddy shedding in Mount Hope Bay and Narragansett Bay: an application of FVCOM. *Journal of Geophysical Research* 111, C10, C10015.